Acta Metallurgica, Vol. 26, pp. 951–962. Pergamon Press, 1978. Printed in Great Britain

A MODEL FOR THE FORMATION OF ANNEALING TWINS IN F.C.C. METALS AND ALLOYS

MARC A. MEYERS

Department of Metallurgical Engineering, South Dakota School of Mines and Technology, Rapid City, SD 57701, U.S.A.

and

LAWRENCE E. MURR

Department of Metallurgical and Materials Engineering, New Mexico Institute of Mining and Technology, Socorro, NM 87801, U.S.A.

(*Received* 25 *April* 1977; *in revised form* 20 *October* 1977)

Abstract—A model for the formation of annealing twins in f.c.c. metals and alloys is proposed. According to it, annealing twin formation proceeds in two stages: initiation and propagation. Initiation takes place at grain boundary ledges. After 'popping out' of the grain boundary, the twin grows into the grain by the migration of the noncoherent twin boundary, that can be represented by an array of partial Shockley dislocations with total Burgers vector equal to zero. Since the twin 'pops out' of the bondary and grows into the grain, the model does not require associated migration of the existing grain boundaries. The twinned region is separated from the grain by means of two parallel coherent twin boundaries. There are two relative orientations of adjacent grains for which the model can operate: (a) when they are at twin orientation (but the boundary is not a coherent twin boundary) and (b) when they are amenable to forming a 'special' boundary. Experimental evidence supporting the model is presented.

Résumé—On propose un modèle pour la formation des macles de recuit dans les métaux et alliages c.f.c. D'après ce modèle, la formation des macles de recuit se produit en deux étapes: la germination et la propagation. La germination se produit aux marches des joints de grains. Après avoir jailli du joint de grains, la macle se propage dans le grain par la migration du joint de macle non cohérent, que l'on peut représenter par un alignement de dislocations partielles de Shockley, dont le vecteur de Burgers total est égal à zéro. Puisque la macle s'échappe du joint de grains et se propage dans le grain, notre modèle ne nécessite pas la migration associée des joints de grains existants. La macle est séparée du grain par deux joints de macles cohérents parallèles. Le modèle peut s'appliquer pour deux orientations relatives des grains adjacents: (a) quand ils sont en relation de macle (mais le joint n'est pas un joint de macle cohérent) et (b) lorsqu'ils peuvent former un joint 'spécial'. On présente des résultats expérimentaux en faveur de ce modèle.

Zusammenfassung—In der Arbeit wird ein Modell für die Bildung von Erholungszwillingen in k.f.z. Metall-Legierungen vorgeschlagen. Danach läuft die Bildung in zwei Stufen ab: Einsetzen und Entwicklung. Einsetzen findet an Vorsprüngen von Korngrenzen statt. Nach dem Ausstoßen aus der Korngrenze wächst der Zwilling durch Wanderung der nichtkohärenten Zwillingsgrenze, welche durch eine Anordnung von Shockleyschen Partialversetzungen mit mit dem Gesamtburgersvektor Null dargestellt werden kann, in das Korn hinein. Da der Zwilling aus der Korngrenze herausgestoßen wird und in das Korn hineinwächst, erfordert das Modell keine Mitwanderung der existierenden Korngrenzen. Der verzwillingte Bereich ist durch zwei parallele kohärente Zwillingsgrenzen gegen das Korn abgetrennt. Für zwei gegenseitige Orientierungen aneinandergrenzender Körner kann der Modellprozess ablaufen: (a) wenn die Körner in Zwillingsorientierung liegen (die Trennfläche aber keine kohärente Zwillingsgrenze ist) und (b) wenn sie zu einer 'speziellen' Grenze führen. Experimentelle Hinweise zur Unterstützung des Modelles werden vorgelegt.

1. INTRODUCTION

The origin and formation of annealing twins in f.c.c. metals and alloys has been a matter of some speculation and numerous attempts have been made [1–16] to explain the formation and growth of annealing twins as distinct from deformation twins. These attempts have taken the form of models or theories of various kinds which have been supported in whole or in part by application to recrystallization and grain growth phenomena or by various other experimental evidence. Most of them can be grouped into three distinct concepts:

(a) Growth accident [1, 8, 10, 13–16]. A coherent twin boundary forms at a migrating grain boundary due to a growth accident.

(b) Grain encounter [4, 6, 12]. Different grains, initially separated, touch each other due to grain growth. If they happen to have twin orientation, the boundary between them will orient itself so that it becomes a coherent twin boundary.

(c) Nucleation by stacking faults and fault packets in migrating grain boundaries and growth through motion either of the grain boundary, leaving behind a parallel-sided twin, or by the combined motion of the noncoherent twin boundary and the grain boundary in opposing directions [11].

Many previous papers dealing with the formation of annealing twins seem to have one particular feature in common. They all point out the inability of any or even combinations of theories to explain all observed phenomena concerned with annealing twins. It is the objective of this paper to propose a model for the formation of annealing twins that does not require associated grain boundary migration; the annealing twin 'pops out' of the grain boundary and grows by glide of a regular array of partial dislocations that comprise the noncoherent boundary, forming in the process two parallel coherent boundaries. The partial dislocations are emitted from grain-boundary ledges.

2. PROPOSED MODEL

For clarity, the twin formation is divided in two stages: initiation and propagation. They will be described separately in Sections 2.1 and 2.2. Section 2.3 presents an atomistic mechanism for annealing twin formation, while Section 2.4 deals with the role of grain boundary ledges in initiation.

Since the proposed model is based on the assumption that the annealing twins 'pop out' of the grain boundary, it has to be atomistically and energetically consistent with the present understanding of grain boundaries. The energy of a boundary [17] depends on both the relative orientation between the grains (characterized by three parameters) and the inclination of the boundary (2 parameters). Chalmers [18] added to these parameters taking into account translation. A plot of grain-boundary energy vs θ, where θ is one of these parameters (the others remaining constant) is cusped. The early rationalizations for these cusps were the 'lattice coincidence' [19] and 'boundary coincidence' concepts [20, 21]. Then came a model emphasizing short, periodic atomic configurations: the 'periodicity concept' [22, 23]. Recent experimental results [24, 25] show incontrovertibly that these 'special boundaries' exist and that the energy depends not only on the relative orientation of the grains, but *also* on the boundary inclination. Among the 'special boundaries' the coherent twin boundary is the one having lowest energy; it has a one to three lattice coincidence and a one to one boundary coincidence.

2.1 *Annealing twin initiation*

According to the present model, there are basically two relative orientations of the adjacent grains for which the conditions for annealing twin formation are satisfied. These two situations will be analyzed separately.

2.1.1. *Adjacent grains at twin orientation.* When the adjacent grains are close to twin orientation and the boundary between them is at random inclination, the grain boundary energy is close to that of a random boundary. If considered alone, the boundary AB between grains A and B might be in an off-equilibrium position, since a convenient change in inclination would rotate it into coherent twin position, with a substantial decrease in its energy. One of these orientations is indicated by a dashed line in Fig. 1(a). Based on this criterion, why wouldn't this boundary already be in such a position? For two reasons:

(a) Considering the ideal grain in a polycrystalline metal as a tetrakaidecahedron [26, 27], each face will have, on the average, five sides (four and six). Therefore each grain boundary is, on the average, in direct contact with 20 other grain boundaries. So, if grain boundary AB (Fig. 1a) rotates, it will affect the areas and orientations of twenty other grain boundaries. In other words, what is good for AB is not necessarily good for all twenty. The minimization of energy criterion has to be applied to the entire system.

(b) If the material was previously cold worked, the relative orientations of the grains are changed. This texture introduced by deformation certainly brings some of the adjacent grains to twin orientation; however, the boundaries between them are not coherent twin boundaries. Thermal activation at ambient temperature is not sufficient to overcome the barriers and change the boundary inclination for most systems.

Assuming then that the situation depicted in Fig. 1 presents itself, a twin nucleus will form when the boundary portion $\overline{12}$ is replaced by a portion $\overline{13}$ and a portion $\overline{23}$, with $\overline{23}$ characterizing the coherent {111} boundary portion (see Fig. 1b). Since $\overline{13}$ represents the noncoherent interface of an incipient annealing twin having interfacial free energy γ_{TB}, $\overline{23}$ represents the coherent twin boundary portion (coincident with {111}) with energy γ_{tb}, and $\overline{12}$ represents the grain boundary portion having an energy γ_{gb}, we can write:

$$(\gamma_{TB} A_{TB} + \gamma_{tb} A_{tb}) < \gamma_{gb} A_{gb}, \tag{1}$$

A_{TB}, A_{tb} and A_{gb} represent the areas of the interfaces corresponding to the segments $\overline{13}$, $\overline{23}$ and $\overline{12}$ respectively. Equation (1) is easily satisfied for small twin nuclei because γ_{TB} varies from about $0.25\,\gamma_{gb}$ to $0.80\,\gamma_{gb}$ and γ_{tb} varies from roughly $0.01\,\gamma_{gb}$ to $0.04\,\gamma_{gb}$ for such common metals and alloys as Cu, Cu–Al alloys, Ni, and stainless steels [28]. Also, the twin nucleus will choose to form, among the various alternatives, in a direction such that $A_{TB} < A_{gb}$, as shown in Fig. 1(a). Since γ_{tb} has such a low energy, A_{tb} is not so important. If the incipient twin is forming during recovery—and it could, since the present model does not require any associated grain boundary migration—the dislocations will be swept out in the twinned region with an additional energy gain term. This energy term would be equal to the product $E_d \rho V$, where E_d is the energy associated with a unit

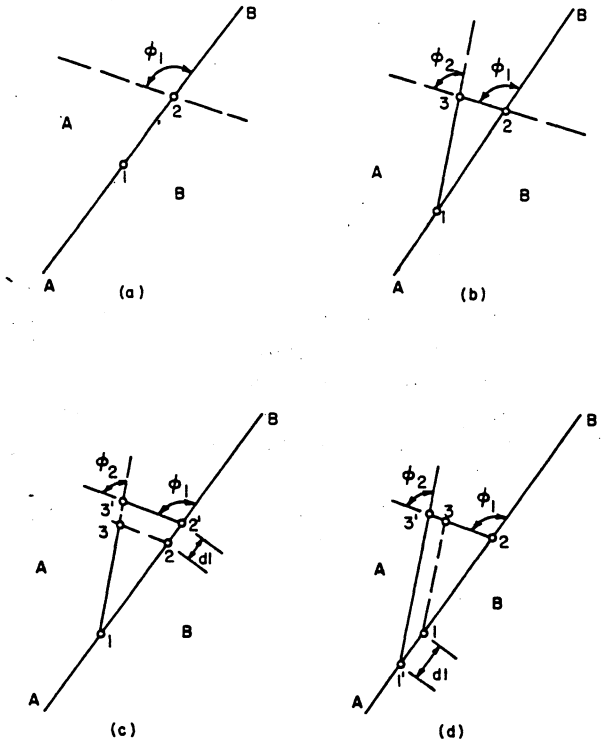

Fig. 1. Schematic representation of initiation of twin formation when the adjacent grains A and B have twin orientation. (a) Grain boundary segment before the formation of a twin nucleus. (b) Decomposition of boundary $\overline{12}$ into a noncoherent boundary $\overline{13}$ and a coherent boundary $\overline{23}$. (c) and (d) Thickening of the nucleus by transport of defects from original to new boundaries.

length of dislocation, ρ is the original dislocation density and V is the volume of the incipient twinned region. This energy, added to equation (1) shows that the driving energy for the formation of the annealing twin would be still higher if dislocation sweep-out is to occur.

While the angle ϕ_1 in Fig. 1 is related to the asymmetry of the grain boundary plane [28], ϕ_2 can be determined from equation (1), or it can be established by the particular coincidence relationships which are known to occur for noncoherent boundaries in Cu [29], Al [30], Ni–Fe alloys [11], and stainless steel [28, 31]. These coincidence relationships will not be entirely achieved in the initiation stage, however; the growth stage will be responsible for rotating the noncoherent boundary into these positions (see Section 2.2).

The length $\overline{13}$ (Fig. 1) derived from the base length $\overline{12}$ is determined by the energy necessary to carry one portion, dA, through the distance $\overline{23}$ by means of either dislocation motion or vacancy migration or both. A specific mechanism showing how the glide of a special array of partial dislocations can create the twin nucleus will be proposed in Section 2.3. These dislocations 'pop out' of the boundary, thus forming the nucleus. For the purpose of the following calculations it suffices to say that a number n of dislocations per unit length of boundary are responsible for the increase in twin nucleus width. The work needed per unit thickness to transport defects from the old boundary portion $\overline{12}$ to the new boundary can be expressed by

$$dW = n \cdot dl \cdot \tau_{PN} \cdot \overline{23}, \tag{2}$$

where τ_{PN} is, to a first approximation, the Peierls–Nabarro stress to move each individual dislocation and dl is an incremental length as noted in Fig. 1(c). In equation (2) it is assumed that the dislocation lengths in the Peierls–Nabarro stress are taken parallel to the dimensions considered for dW. The work dW can be equated to the decrease in the total interfacial free energy upon forming a ledge portion acting as a twin nucleus, (with reference to equation 1 and Fig. 1) in the absence of dislocation sweep-out. Substituting equation (2) for dW, one has:

$$n \cdot dl \cdot \tau_{PN} \cdot \overline{23} = \gamma_{gb}\, dl - \gamma_{TB}\, dl \frac{\sin\phi_1}{\sin\phi_2} - \gamma_{tb}\, dl \frac{\sin(\phi_1 - \phi_2)}{\sin\phi_2}. \tag{3}$$

If the angles ϕ_1 and ϕ_2 are known, the width of the twin nucleus can be determined, because the triangle $\overline{123}$ is perfectly determined by knowing θ_1, ϕ_2 and $\overline{23}$. So:

$$\overline{12} = \frac{1}{\tau_{PN}} \cdot \frac{\gamma_{gb}}{n \cdot \cos(\phi_1 - \phi_2)} \times \left[1 - \left(\frac{\gamma_{TB}}{\gamma_{gb}}\right)\sin\phi_1 - \left(\frac{\gamma_{tb}}{\gamma_{gb}}\right)\sin(\phi_1 - \phi_2)\right]. \tag{4}$$

Assuming, as a first approximation, that the grain-boundary energies and angle ϕ_2 are temperature independent, the width $\overline{12}$ of the twin nucleus varies with the inverse of the Peierls–Nabarro stress. Since this stress decreases with increasing temperature, due to thermal activation, equation (4) predicts an increase of the twin nucleus width with temperature. An alternative growth of the twin nucleus to reach its equilibrium size is shown in Fig. 1(d). Here the expansion is proceeding through the transport of dislocations at the edge l of the twin changing it to l', and increasing the length $\overline{12}$ in the process. In the above calculations only the energy required to transport dislocations from the 'old' to the 'new' boundary was considered; a more rigorous expression would have to take into account the energy to form the dislocations at the tip of the ledge.

2.1.2 *Adjacent grains amenable to form 'special boundary' after twin formation.* If the two adjacent grains are at a random orientation and the boundary between them is a random boundary, the grain boundary decomposition of Section 2.1.1 no longer takes place. However, it is possible to decrease the overall interfacial energy without changing the position of the boundary AB (Fig. 2). A twin nucleus (with respect to A) is generated. Again, $\overline{23}$ and $\overline{13}$ are the coherent and noncoherent boundaries, with energies γ_{tb} and γ_{TB}, respectively. The random high-energy boundary $\overline{12}$ (with γ_{AB}) is substituted by a new

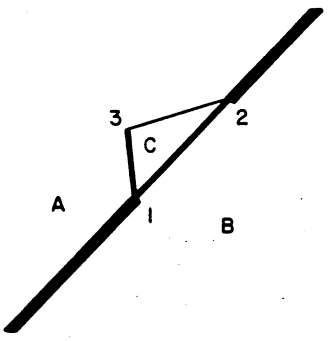

Fig. 2. Initiation of twin formation when the adjacent grains are amenable to form 'special boundary'. Decomposition of boundary $\overline{12}$ into a noncoherent twin boundary $\overline{13}$, coherent twin boundary $\overline{23}$, and a 'special boundary' $\overline{12}$. The thicknesses of the lines have been made approximately proportional to the energies of the boundaries.

boundary $\overline{12}$ (γ_{BC}), since the relative orientations of A and B, and C and B are different. So, a twin nucleus will form if one has, per unit thickness:

$$(\gamma_{tb}\, 23 + \gamma_{TB}\, \overline{13} + \gamma_{BC}\, \overline{12}) < \gamma_{AB}\, \overline{12} \qquad (5)$$

This inequality is only possible if $\gamma_{BC} < \gamma_{AB}$. Since the existence of special boundaries with energies considerably lower than random boundaries is well established (e.g. Ref. 28), the situation shown above is possible. If the relative orientation of grains A and B is such that BC forms a 'special' boundary, the above condition could be satisfied. The other calculations of Section 2.1.1 can be applied, *mutatis mutandis*, to this situation.

2.1.3 *Probability*. One apparent limitation of the model is that the probability of two adjacent grains having exactly twin orientation (Section 2.1.1) or having a relative orientation so that a twin transformation produces a special boundary (Section 2.1.2) is infinitely small. Indeed this so, if *exact* relative orientations are considered. However, the nucleation mechanisms are also appropriate for orientations close to exact orientations. When the two grains are close to twin orientation, the boundary portion $\overline{12}$ (Fig. 1) will not vanish entirely after nucleation. The angular mismatch is absorbed by this boundary, and a tilt, twist or tilt/twist boundary is formed. The energies of these low-angle boundaries increase from zero to the value of random boundaries over a range of several degrees; the initial increase is linear with relative angle between the adjacent grains. So, in this case a special term has to be added to equation (1), which becomes:

$$(\gamma_{TB}\, A_{TB} + \gamma_{tb}\, A_{tb} + \gamma_{la}\, A_{gb}) < \gamma_{gb}\, A_{gb}, \qquad (6)$$

where γ_{la} is the energy of the low-angle boundary. If it is small enough (i.e. if the misorientation angle is small enough) this inequality can be satisfied. The misorientation dependence of energy depends on the material and on the type of low-angle boundary. Some of these are given by Gleiter and Chalmers [17]. If it is assumed that low-angle boundaries having up to 4° misorientation still have low enough energies to satisfy equation (6) and, consequently, provide nucleation sites for annealing twins, it would be instructive to calculate the probability of adjacent grains having a relative orientation within this range. It is assumed, of course, that the grains have random orientation. The probability of one (111) plane being within a 4° range is equal to the probability of its pole being within the solid angle of 4°. This probability is equal to the surface area of the cap divided by the surface area of the sphere, or $P_1 = 0.0012$. The {111} planes, when at twin orientation, have a common ⟨110⟩ direction. The dihedral angle between these planes, in f.c.c. metals and alloys, is 70° 32′ [32]. There are three ⟨110⟩ directions in each {111}; consequently, the probability that a (111) plane in a grain B is at twin orientation with a (111) plane in a grain A, and that they intersect themselves along $[110]_A$ is:

$$P_2 = 2 \times 3 \times 8/360 \times P_1 = 0.00016. \qquad (7)$$

The factor 2 stems from the fact that there are two alternatives for $(111)_B$ to make an angle of 70° 32′ with $(111)_A$ along $[110]_A$; the factor 8/360 comes from the ±4° range assumed; the factor 3 is due to the three $\langle 110\rangle_B$. Since the multiplicity factor of {111} planes is 4, the probability that two adjacent grains A and B are within twin orientation is equal to the probability that any of the {111} planes in both grains are within 4° of twin orientation, and that their ⟨110⟩ directions are within 4° (the factor 3 comes from the multiplicity of $\langle 110\rangle_A$).

$$P_3 = 3 \times 4 \times 4P_2 = 0.00768. \qquad (8)$$

Since each grain has, on the average, fourteen next neighbors [26, 27] the probability P_4 of a grain having a neighbor within 4° of twin orientation is $14P_3$, or 0.108. So, about 10% of the grains have neighbors within 4° of twin orientation, and 10% of the grains are amenable to initiation of twin formation by the model described in Section 2.1.1. If the relative orientation of the grains is not random the probability might be different. For instance, cold work might introduce a texture bringing the {111} closer to their 70° 32′ twin orientation. This would result in an increase in the probability P_4.

For the case in which the adjacent grains are amenable to special orientation by twinning (Section 2.1.2) the same reasoning can be applied. Since the number of orientations producing special boundaries is much greater than the ones producing twin boundaries (e.g. Herrman *et al.* [24], the chances for twin nucleation for this configuration are much larger.

2.2 *Annealing twin propagation*

The twin nucleus is depicted tri-dimensionally in Fig. 3(a). It traverses the AB boundary entirely, and its limiting faces $\overline{123}$ and $\overline{456}$ are in direct contact with the adjoining grains C and D, respectively. $\overline{2365}$ and $\overline{1463}$ are the coherent and non-coherent twin

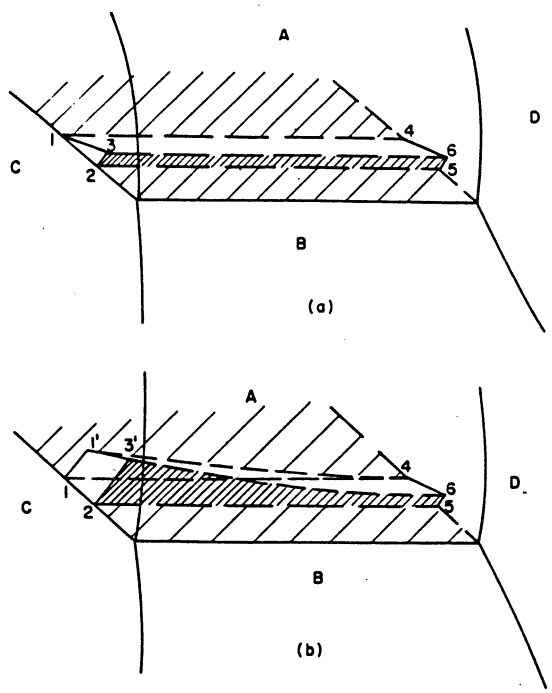

Fig. 3. Three-dimensional representation of twin nucleus and incipient twin formation which appears as a ledge or double ledge in the grain boundary plane. (a) Small triangular nucleus as in Fig. 1(b). (b) Popping out of incipient twin along one portion of the grain boundary to form a partially grown annealing twin band.

boundaries, respectively, and the original boundary $\overline{1254}$ has vanished, or has been substituted by a 'special boundary'. The growth of the twin from its nucleus will proceed through the migration of the noncoherent twin boundary $\overline{1463}$, as shown in Fig. 3(b). Again, the driving energy for the process will be the reduction of the overall interfacial energy and dislocation density (if recovery has not been completed). The energy of the noncoherent twin boundary depends on its inclination. By rotating it conveniently, it will fall into one of the 'special boundary' orientations (see Section 2.1). Indeed, the noncoherent twin boundaries have been found to have preferential orientations. The energy gradient provides a torque that tends to rotate the noncoherent twin boundary away from its nucleus inclination. Fullman [29] found that it is approximately parallel to a {113} plane of one crystal and to a {335} plane of the other. Other ivestigators [11, 28, 30, 31] have alsc found preferential orientations. Figure 3(b) shows the growth of the twin under the influence of the combined driving energies. The growth takes place by migration of the noncoherent twin boundary parallel to {111}; this assures a relatively low energy expenditure in the formation of the lateral boundaries $\overline{23'65}$ and $\overline{11'4}$, since they are coherent twin boundaries. However, the separation between the parallel coherent boundaries is not expected to change during the propagation stage; it is thought [8, 34] that the mobility of coherent twin boundaries in a direction perpendicular to the boundary is much lower than that of random boundaries. If the growth is taking place during recovery, the sweep-up inside the twinned volume provides a source of driving energy. The growth will be completed when a minimum level of energy is reached. Figure 4 shows how this tri-dimensional twin will appear in a micrograph; depending on the sectioning planes, different morphologies are observed.

Since the noncoherent twin boundary represents the interface between two lattices with high coincidence (one in three) it is a low energy boundary even when it is not exactly at a 'special orientation'. Measurements of the noncoherent grain boundary energy systematically show lower energies than random grain boundaries [28, 29]. Aust and Rutter [33–35] showed, for pure lead, that while the migration rates of random and special boundaries were identical, the addition of small amounts of tin affected the migration rates of random boundaries much more than special boundaries. The results indicate that the solute atoms segregate more in the random than in the special boundaries, hindering the mobility of the former ones. Evidence for this preferential segregation at random boundaries is presented by Gleiter [36]. It can be concluded from the above that the noncoherent boundary $\overline{23}$, once it 'pops out' of the grain boundary (see Figs. 1 and 2), has a higher mobility than the surrounding grain boundaries. Its migration —and the associated twin propagation—could therefore proceed at temperatures below the recrystallization temperature.

2.3 *Atomistic mechanism*

The normal {111} stacking sequence in f.c.c. metals and alloys is altered by twinning. A parallel-faced twin could be represented by the sequence: $\ldots A\ B\ C\ A\ B\ \overline{C}\ B\ A\ C\ B\ A \ldots A\ C\ B\ \overline{A}\ B\ C\ A\ B\ C \ldots$ The $\overline{A}$ and $\overline{C}$ planes act as mirror planes. The formation of the twinned region enclosed by the twinning planes can be rationalized by means of defect movement. Since the annealing twins are not generated in response to mechanical stresses, no shear strain should be involved and the dislocation mechanisms proposed for mechanical twins (e.g. Ref. 37) are not appropriate. A mechanism has been proposed by Votava and Berghezan [38], but it is not applicable to the present situation; an alternate mechanism is presented in Fig. 5. The noncoherent boundary is formed by a regular array of Shockley dislocations. These dislocations 'pop out' of the boundary and propagate into the material. Their arrangement is such that they (a) change the normal to twin stacking sequence and (b) introduce minimal strain in the material. They are associated pairwise with opposite signs, forming dipoles. Since the {111} planes labelled C are not affected by twinning, there is no need for dislocations in them. The strain energy of the individual dislocations within the dipoles is minimized if they position themselves at an angle in the vicinity of 45° as shown in Fig. 5. They attract themselves to that position. The relative position of the dipoles will also be such as to minimize the energy. This

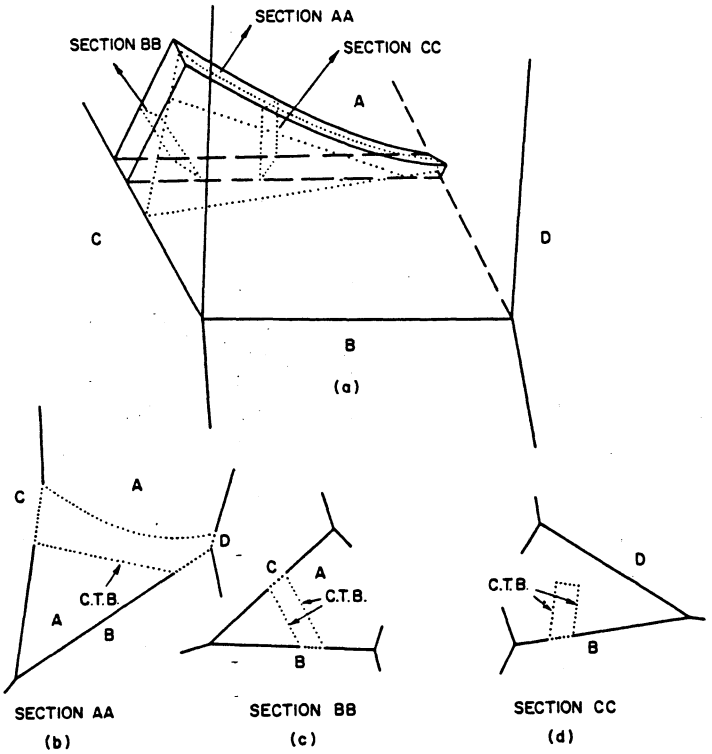

Fig. 4. Three-dimensional view of partially grown annealing twin band and morphologies it can take depending on the sectioning plane. (b) Grain-corner twin, if sectioning plane is *AA*. (c) Complete parallel-sided twin, if sectioning plane is *BB*. (d) Incomplete parallel-sided twin, if sectioning plane is *CC*.

energy minimum should coincide with the 'special' boundary inclination. It can be observed in Fig. 5 that the net Burgers vector of all partial dislocations in the noncoherent boundary is equal to zero; this shows that the strain energy associated with them is minimal.

2.4 *The role of grain-boundary ledges*

There are several important aspects in recognizing a twin nucleus as either a grain boundary ledge or of possessing ledge character. Since individual pure ledges are already recognized to be sources of dislocations and stacking faults during deformation [28], there is no reason they cannot be nuclei for twin formation. Indeed, Kinsman *et al.* [39, 40] observed stacking faults and κ plates (h.c.p.) formed from grain-boundary ledges in the Cu–Si system by means of dislocations 'popping out' from ledges and moving into the grains (Fig. 18 of Ref. 40). Kennedy *et al.* [41] observed a phase transformation in cobalt by dislocation emission from grain boundaries. Consequently, a grain boundary ledge can provide a simple means of explaining annealing twin formation at a grain boundary. It can explain the variations in twin formation in the presence of strain energy, and it can account for the role stacking faults, twin-faults, and deformation twins have apparently played in the observations of the formation of annealing twins [1–3, 5, 7, 8, 11]. Since grain-boundary dislocations and ledges may glide and pile up at a grain-boundary triple junction [28, 55] the formation of grain corner twins [10] is also easily accounted for, and the role of stacking faults even in the nucleation of an annealing twin at a grain corner can be recognized as a simple feature of a ledge. That ledges are associated with the twin orientation {111} is well known [28]. Figure 6 illustrates the appearance of ledges in nickel

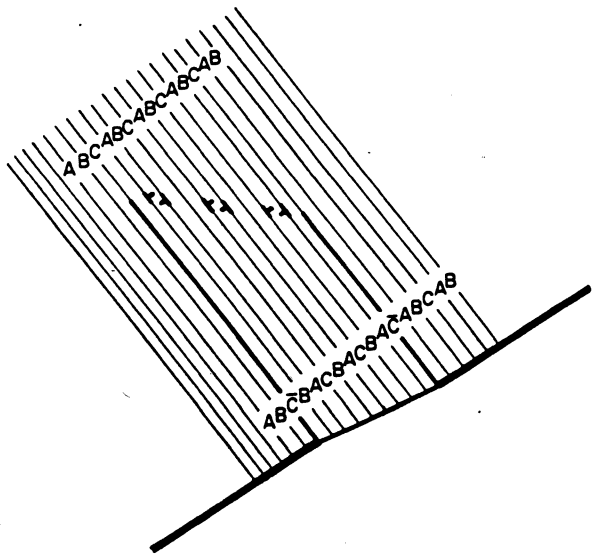

Fig. 5. Atomistic representation of annealing twin growth by the movement of partial dislocations on {111}. Note that the partial dislocations form pairs of opposite sign so that only small amounts of material are moved away from the original boundary.

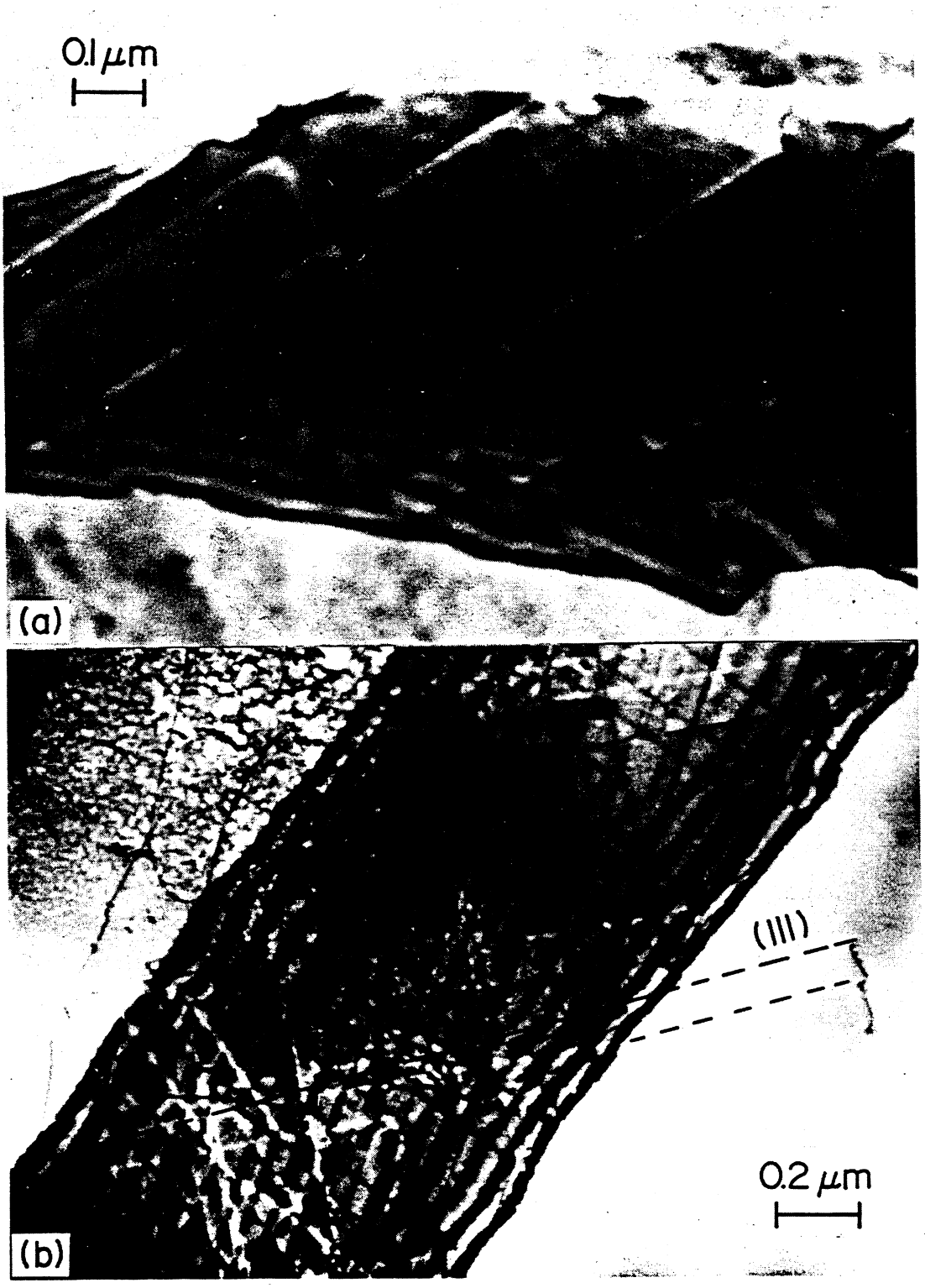

Fig. 6. Examples of ledges of varying dimensions in the grain boundaries of nickel films imaged in the transmission electron microscope. (a) Large ledges are readily observed by the boundary fringe displacements. (b) 'Families' of smaller ledges which are coincident with the {111} planes of one or the other grains separated by the interface.

grain boundaries as observed in the transmission electron microscope. Figure 7 shows several examples of ledges acting as sources of dislocations in a low-stacking-fault energy material where the dislocations have split into partials connected by a stacking fault.

3. EXPERIMENTAL SUPPORT AND DISCUSSION

There is a considerable body of indirect evidence which lends support to the proposals contained in this paper. It is presented in items (a)–(g) below.

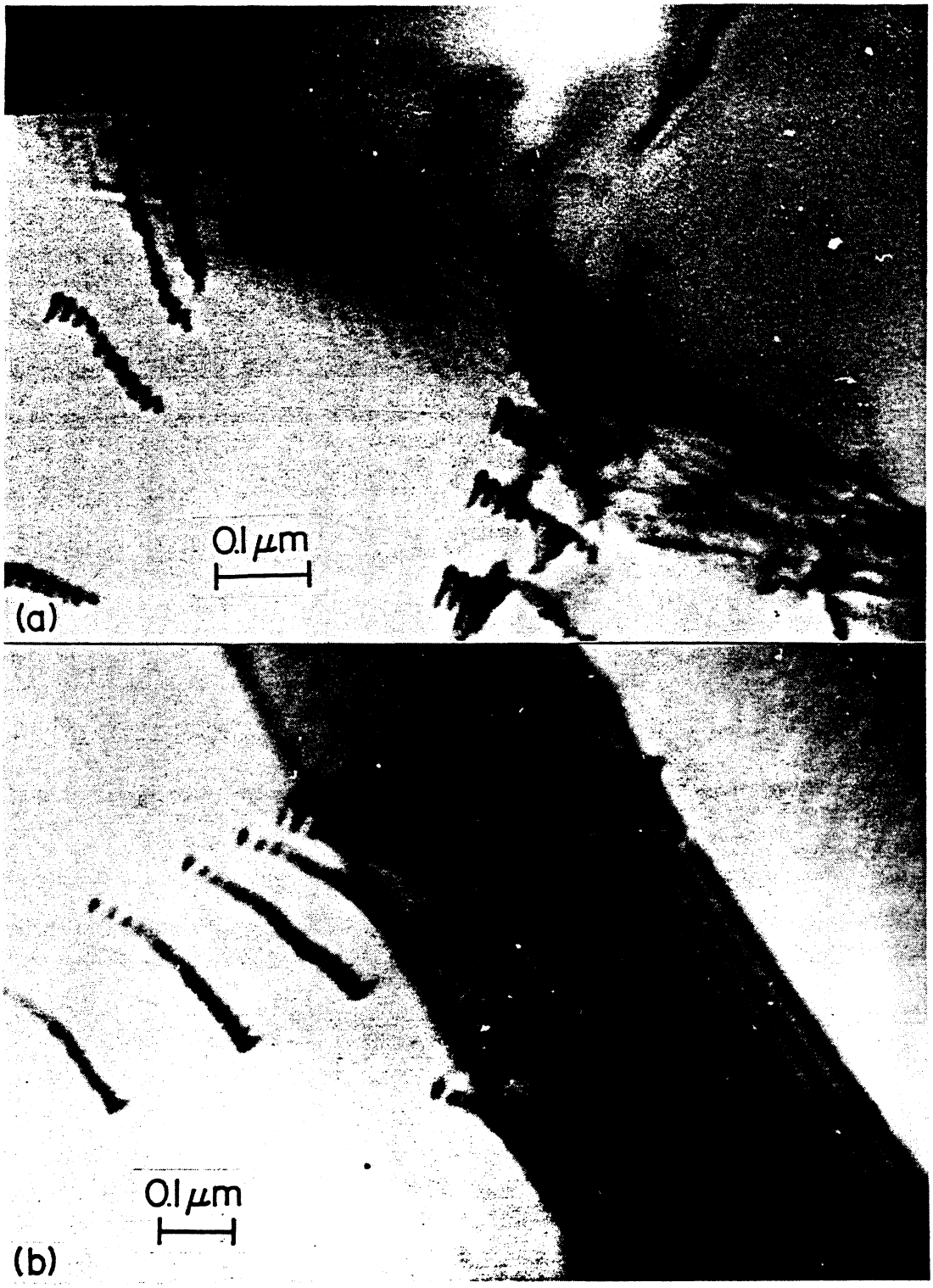

Fig. 7. Dislocations and stacking faults emitted at grain boundary ledges in 304 stainless steel. (a) Closely-spaced ledges coincident with (111) planes. Only particular ledges are observed to be operative. (b) Partial dislocations separated by stacking faults emitted at a large grain boundary ledge during observation in the electron microscope.

(a) Examples of stacking faults nucleating at ledges have been observed. Figure 8 illustrates the formation of several overlapping stacking faults at a ledge or ledges during the observation of the thin foil area in the transmission electron microscope. The dark-field image shows conclusively the formation of thin twinned regions where stacking faults overlap on every (111) plane.

(b) Figure 9 shows schematically the three typical morphologies at annealing twins encountered in f.c.c. metals. *A* is a grain-corner twin, while *B* is a complete and *C* an incomplete parallel-sided twin. If the ratio

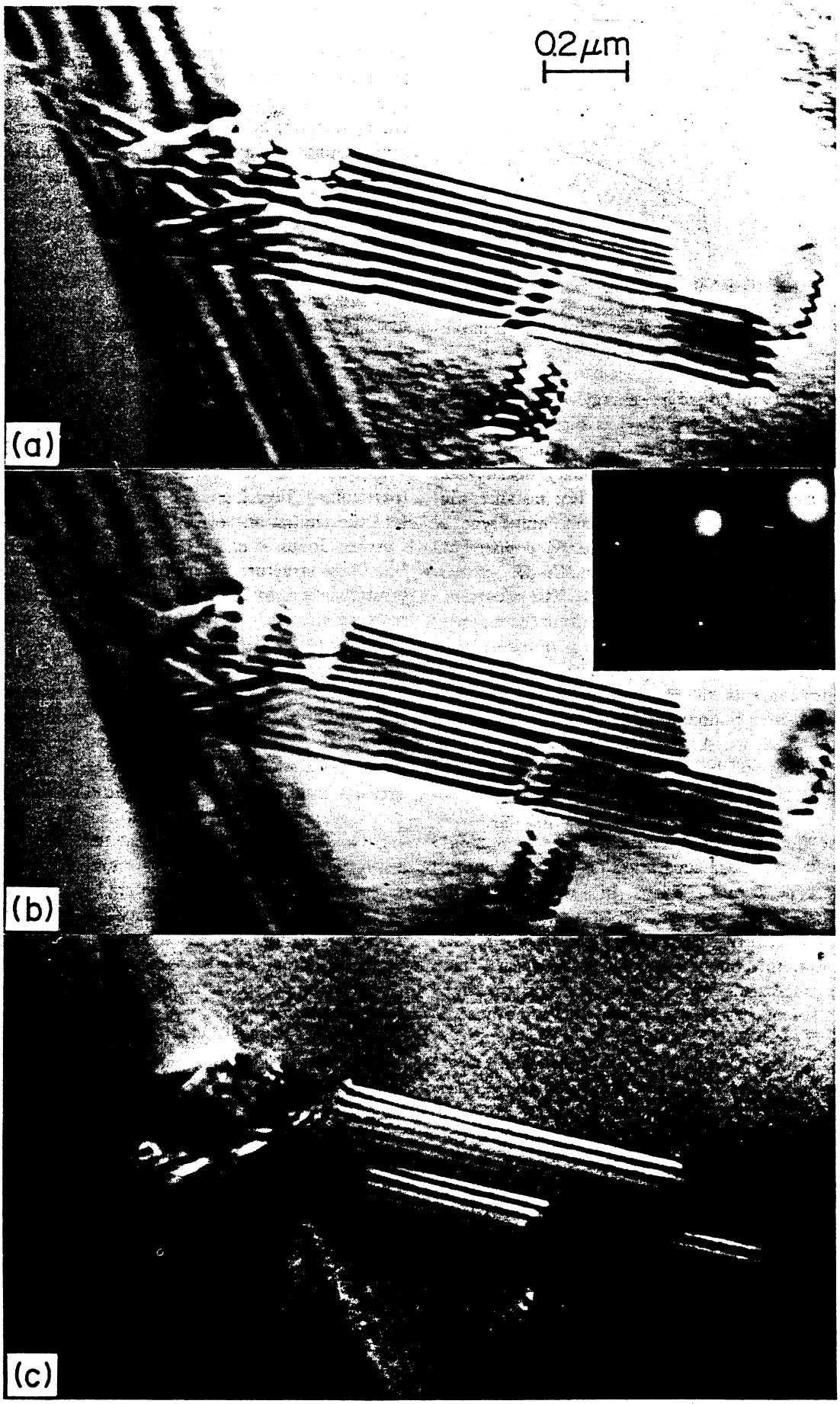

Fig. 8. Long, extended stacking faults emitted at a ledge or ledges in a grain boundary in stainless steel while being examined in the transmission electron microscope. (a) Overlapping stacking faults emitted on closely-spaced (111) planes. (b) Bright-field transmission electron microscope image similar to (a) but tilted for 2-beam diffraction with [111] operating reflection shown in selected-area electron

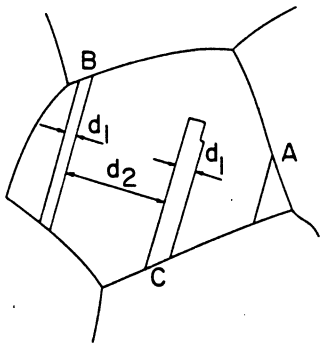

Fig. 9. Three types of annealing twin morphologies observed in f.c.c. metals and alloys. *A* is a grain corner twin; *B* is a complete parallel-sided twin; *C* is an incomplete parallel-sided twin.

of coherent twin boundary energy with respect to grain boundary energy (γ_{tb}/γ_{gb}) is high only type *A* twins are observed; lowering of this ratio will result both in an increase of twin boundary density and formation of types *B* and *C* twins. For instance, aluminum [42] ($\gamma_{tb}/\gamma_{gb} = 0.23$) exhibits only type *A* twins, while nickel [43] ($\gamma_{tb}/\gamma_{gb} = 0.049$), copper [44] ($\gamma_{tb}/\gamma_{gb} = 0.035$), the Cu–Sn, Cu–Zn, Cu–Ga systems exhibit the three types of twins [10]. The occurrence of type *B* and *C* twins—which constitute the majority of twins in systems with low γ_{tb}/γ_{gb} ratios—cannot be explained by either the growth accident or grain encounter concepts; the original explanation was that the two coherent boundaries are formed by successive *independent* events. A strong argument against this explanation would be: if the parallel coherent boundaries in type *B* and *C* twins are formed by independent events during grain growth or recrystallization, then the mean distance between different twin should be equal to the mean separation between the parallel sides in type *B* and *C* twins. In Fig. 9 this would mean that, on the average $\overline{d_1} = \overline{d_2}$; a visual inspection of any f.c.c. metal or alloy with low γ_{tb}/γ_{gb} ratio shows that this direct relationship between d_1 and d_2 does not exist. Only the model herein presented is simultaneously able to explain the occurrence of type *A*, *B*, and *C* (Fig. 9) twins.

(c) Bäro and Gleiter [15] determined the density of annealing twins formed during grain growth as a function of grain size and temperature (450–750°C) for a Cu–3 wt.%Al alloy. While for annealing temperatures above 600°C the experimental results agreed quantitatively with the growth accident model, at lower temperatures the observed twin densities were much higher than the ones predicted by the model. Bäro and Gleiter [15] suggested that the disagreement could be due to another (or an additional) annealing twin formation mechanism operating in the 450–600°C range.

(d) The change in grain-boundary orientation at the intersection with twins of type *B* and *C* (Fig. 9) is well known; interfacial angles at these intersections have been used to determine the energy ratios γ_{tb}/γ_{gb} [15, 28, 44, 45]. This change in orientation has been variously interpreted as due to the fact that only partial equilibrium is achieved at the junctions [44, 45], and that interfacial torques [43] were acting on the junctions. An alternative explanation for the change in orientation, in line with the idea that the interfacial energy depends both on grain misorientation and on grain-boundary tilt, is that the grain-boundary portion between the parallel twin boundaries (region $\overline{12}$ in Figs. 1 and 2) is a 'special boundary'. Being at the bottom of an energy cusp, its orientation is fixed.

(e) Decerf *et al.* [46], upon studying the recrystallization of deformed nickel, present two photographs that illustrate strikingly the proposed model (Figs. 1 and 14 of Ref. 46). Recrystallized grains, having nucleated at grain boundaries, grow and have the form of incomplete parallel-sided twins.

(f) The observations by Vaughan [31] (particularly, Figs. 1 and 3 of that reference) as well as the dissociation of boundaries described by Ashby and Harper —as quoted in Ref. 13— and by Goodhew [47, 56] (particularly, Figs. 2 and 4 of Ref. 56) provide support for the initiation of annealing twin formation. Further, Jones *et al.* [48] observed changes in grain boundary structure during the earliest stages of recrystallization, and suggested that a link could exist between boundary recrystallization and the formation of nuclei for general recrystallization.

(g) It has been shown by Venkatesh and Murr [49] and Murr and Venkatesh [50] that the density of ledges (number per unit length of grain boundary) can be altered by thermomechanical treatment, and it has been observed to increase generally with increasing cold reduction. If the grain-boundary ledge density represents some constant proportion of potential twin nuclei (as for example the ratio of nuclei with twin orientation to the number with matrix orientation as defined by Gleiter [13], then it would follow that as the ledge density increases, the twin nuclei would increase. As a means to more directly check the previous argument, the experimental data of Murr and Venkatesh [50] for nickel were reexamined in more detail. In particular, the samples for which the ledge density had been systematically increased by cold reduction and annealing treatments were electropolished and examined in a Vickers metallograph. The coherent twin boundaries were measured in terms of total length of coherent twin boundary per unit area of specimen surface for each cold-reduction treatment, and the results compared with the ledge densities as shown in Fig. 10. These results indicate that the twin density increases with an increase in grain boundary ledge density for a constant grain size. The effects of grain size and prior cold work as discussed by Gindraux and Form [16] on twin formation are therefore related to ledge density and not dislocation density as they concluded. Although the results shown in Fig. 10 do not prove incontrovertibly the proposed model, they indicate a relationship between ledge and annealing twin density. Alternative explanations would be (a) the differ-

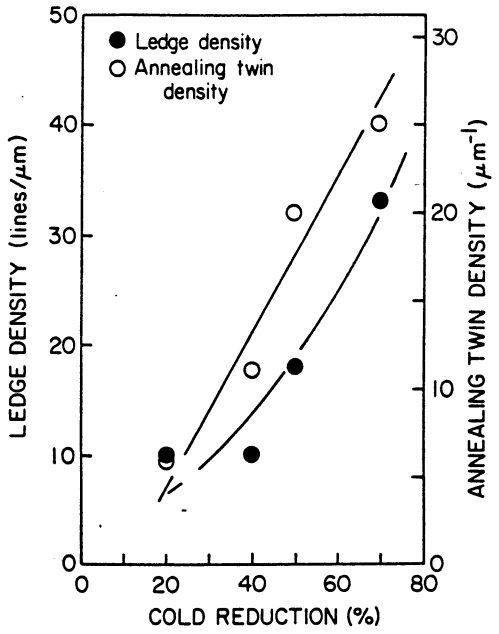

Fig. 10. Comparison of measured density of annealing twins and grain boundary ledge density as a function of percent cold reduction in nickel. Initially mill-rolled and annealed sheet was stress-relief annealed 5 min at 300°C, rolled as indicated, and finally annealed at 750°C for times of 2, 3, 4 and 5 min for the respective cold-reduction schedule to produce a constant grain size of approximately 30 μm.

ences in texture in the different samples and (b) different cold-rolling reductions producing differences in recrystallization.

It is recognized that the extension of the annealing twin model herein presented to deformation twins would be somewhat speculatory. However, one has to recognize the similarities between both types of twin. The nucleation sites for deformation twinning could also be provided by grain-boundary ledges; the noncoherent boundary would however be composed of an entirely different dislocation array [15, 52]. Grain boundary ledges can provide support for deformation twin production of grain boundaries involving overlapping stacking faults and the like [53, 54]. While, as shown in Figs. 7 and 8, it is a relatively simple matter to obtain direct evidence which supports the contention that grain boundary ledges can act as sources of stacking faults and twin-faults in f.c.c. materials, it is much more difficult to demonstrate the formation of thicker and better-defined deformation twins. The reason for this shortcoming is recognized to be associated with the usually large stresses or strains required to initiate well-defined deformation twins.

4. SUMMARY AND CONCLUSIONS

(a) A model for the formation of annealing twins is proposed. According to it an annealing twin 'pops out' of the grain boundary and propagates in the grain by means of the migration of the noncoherent twin boundary.

(b) Contrary to previous models, this one does not require any associated grain boundary migration for the formation of the annealing twins. The driving energy for annealing twin formation according to the model is the overall reduction of dislocation density and interfacial energy.

(c) The model predicts the formation of the annealing twins in two stages: initiation and propagation.

(d) Initiation takes place under two circumstances:

(i) two adjacent grains are at twin orientation, but the boundary is a random boundary (Fig. 1).

(ii) two adjacent grains are amenable to form a 'special boundary' by twinning. This 'special boundary' has a lower energy than a random boundary (Fig. 2).

It is demonstrated that there is a substantial probability for two adjacent grains to have relative orientations close to (a) and (b) above.

(e) Propagation of the twin nucleus proceeds by the migration of the noncoherent boundary into the grain (Fig. 3). The noncoherent boundary can be represented by an array of parallel Shockley dislocations, as shown in Fig. 5. The total Burgers vector of the boundary is zero, and the amount of strain introduced by it is minimal. No atom has to move by a distance larger than one interatomic spacing to form the twinned region. The noncoherent boundary will propagate until the total system (noncoherent plus coherent boundaries) achieves a position of lowest energy.

(f) It is suggested that the initiation of annealing twins takes place at grain-boundary ledges. Evidence favoring this mechanism is given by the fact that for nickel, the annealing twin density increases with ledge density, at a constant grain size. Further support for the model found in the literature is presented.

(g) It is suggested that grain-boundary ledges could also act as nucleation sites for deformation twins.

Acknowledgements—We wish to thank Professor C. S. Barrett, University of Denver, and Dr. A. Pattnaik, Drexel University, for stimulating discussions and comments on the manuscript.

REFERENCES

1. H. Carpenter and S. Tamura, *Proc. R. Soc.* (A) **113**, 161 (1926).
2. C. H. Mathewson, *Proc. Inst. Metals Div., A.I.M.E.* **7**, 1928 (1928).
3. C. H. Mathewson, *Trans. Am. Soc. Metals* **32**, 38 (1944).
4. W. G. Burgers, *Nature, Lond.* **157**, 76 (1946).
5. J. E. Burke and Y. G. Shiau, *Trans. A.I.M.E.* **175**, 141 (1948).
6. W. G. Burgers, *Physica* **15**, 92 (1949).
7. R. Maddin, H. Mathewson and R. Hibbard, *Trans. A.I.M.E.* **185**, 655 (1949).
8. J. E. Burke, *Trans. A.I.M.E.* **188**, 1324 (1950).
9. Discussion of ref. 7, *Trans. A.I.M.E.* **188**, 1020 (1950).
10. R. L. Fullman and J. C. Fisher, *J. appl. Phys.* **22**, 1350 (1951).

11. S. Dash and N. Brown, *Acta Met.* **11,** 1067 (1963).
12. J. P. Nielsen, *Acta Met.* **15,** 1083 (1967).
13. H. Gleiter, *Acta Met.* **17,** 1421 (1969).
14. P. Merklen, E. Furubayashi and H. Yoshida, *Trans. Japan Inst. Metals* **11,** 252 (1970).
15. G. Bäro and H. Gleiter, *Z. Metallk.* **63,** 661 (1972).
16. G. Gindraux and W. Form, *J. Inst. Metals* **101,** 85 (1973).
17. H. Gleiter and B. Chalmers, *High-Angle Grain Boundaries* (edited by B. Chalmers, J. W. Christian and T. B. Massalski), Vol. 16. Pergamon Press, Oxford (1972).
18. B. Chalmers, *J. less-common Metals* **28,** 277 (1972).
19. M. L. Kronberg and F. H. Wilson, *Trans. A.I.M.E.* **185,** 501 (1949).
20. D. G. Brandon, B. Ralph, S. Ranganathan and M. S. Wald, *Acta Met.* **12,** 813 (1964).
21. D. G. Brandon, *Acta Met.* **14,** 1479 (1966).
22. G. Bishop and B. Chalmers, *Scripta Met.* **2,** 133 (1968).
23. B. Chalmers and H. Gleiter, *Phil. Mag.* **23,** 1541 (1971).
24. G. Herrmann, H. Gleiter and G. Bäro, *Acta Met.* **24,** 353 (1976).
25. H. Sautter, H. Gleiter and G. Bäro, *Acta Met.* **25,** 467 (1977).
26. C. S. Smith, *Metal Interfaces*, p. 65. A.S.M., Metals Park, Cleveland (1952).
27. F. N. Rhines, K. R. Graig and R. T. DeHoff, *Metall. Trans.* **5,** 413 (1974).
28. L. E. Murr, *Interfacial Phenomena in Metals and Alloys*. Addison-Wesley, Reading, Mass (1975).
29. R. L. Fullman, *J. appl. Phys.* **22,** 456 (1951).
30. C. M. Sargent, *Trans. metall. Soc. A.I.M.E.* **242,** 1188 (1968).
31. D. Vaughan, *Phil. Mag.* **22,** 1003 (1970).
32. L. E. Murr, *J. appl. Phys.* **39,** 5557 (1968).
33. K. T. Aust and J. W. Rutter, *Trans. metall. Soc. A.I.M.E.* **215,** 119 (1959).
34. K. T. Aust and J. W. Rutter, *Trans. metall. Soc. A.I.M.E.* **215,** 820 (1959).
35. J. W. Rutter and K. T. Aust, *Trans. metall. Soc. A.I.M.E.* **218,** 682 (1960).
36. H. Gleiter, *Acta Met.* **18,** 117 (1970).
37. A. W. Sleeswyk, *Acta Met.* **10,** 705 (1962).
38. E. Votava and A. Berghezan, *Acta Met.* **7,** 392 (1959).
39. K. R. Kinsman, H. I. Aaronson and E. Eichen, *Metall. Trans.* **2,** 1041 (1971).
40. K. R. Kinsman and H. I. Aaronson, *Metallography* **7,** 361 (1974).
41. E. M. Kennedy, R. Speiser and J. P. Hirth, in *Physical Chemistry in Metallurgy*, p. 345. Darken Conf., U.S. Steel Corp., Pittsburgh (1976).
42. L. E. Murr, *Acta Met.* **21,** 791 (1973).
43. L. E. Murr, R. J. Horylev and W. N. Lin, *Phil. Mag.* **20,** 1245 (1969).
44. R. L. Fullman, *J. appl. Phys.* **22,** 448 (1951).
45. L. E. Murr, P. J. Smith and C. M. Gilmore, *Phil. Mag.* **17,** 89 (1968).
46. J. Decerf, J. Hennaut, R. Pankowski and M. G. Homès, *Mém. scient. Revue Métall.* **70,** 145 (1973).
47. P. J. Goodhew and R. M. Allen, *Scripta Met.* **11,** 37 (1977).
48. A. R. Jones, P. R. Howell and B. Ralph, *Phil. Mag.* **35,** 603 (1977).
49. E. S. Venkatesh and L. E. Murr, *Scripta Met.* **10,** 447 (1976).
50. L. E. Murr and E. S. Venkatesh, *Metallography*. To be published.
51. S. Mahajan and D. F. Williams, *Int. Metall. Rev.* **18,** 43 (1973).
52. S. Mahajan and G. Y. Chin, *Acta Met.* **21,** 1353 (1973).
53. J. B. Cohen and J. Weertman, *Acta Met.* **11,** 997 (1963).
54. H. Fujita and T. Mori, *Scripta Met.* **9,** 631 (1975).
55. J. P. Hirth and R. W. Balluffi, *Acta Met.* **21,** 929 (1973).
56. P. J. Goodhew, in *Grain Boundaries*, p. A.40. (1976 Spring Res. Conf., Jersey). Nortway Ho., London (1976).